Reliability of the tensile force identification in ancient tie-rods using one flexural mode shape

Nerio TULLINI[a], Giovanni REBECCHI[b] and Ferdinando LAUDIERO[c]

[a, c]*Department of Engineering, University of Ferrara, Via Saragat 1, Ferrara, 44100, Italy,*

[b]*Harpaceas S.r.l., Structural and Geotechnical Group, Viale Richard 1, Milan, 20143, Italy,*

[a] Corresponding author: e-mail: nerio.tullini@unife.it

[b] e-mail: rebecchi@harpaceas.it

[c] e-mail: ferdinando.laudiero@unife.it

Abstract

This paper presents an investigation into the reliability of an experimental procedure for the axial load identification of tie-rods with unknown boundary conditions, that uses one vibration frequency and five amplitudes of the corresponding mode shape. The method adopted does not require the knowledge of the effective length of the tie-rod under examination, but only the flexural rigidity and the mass per unit length. In particular, the influence of measurement errors as well as of inaccurate estimates of geometric and elastic properties on the accuracy of the axial force identification is investigated. The effect of the added mass of the sensors is also analyzed. The proposed algorithm is verified by means of many numerical tests on ancient tie-rods having large scatter values of geometric and elastic properties. Good estimates of the axial forces are obtained. Moreover, it is shown that the reliability of the tensile force identification, using one flexural mode shape, relies on the magnitude of the measurement errors rather than on accurate guess of Young modulus.

Keywords

Tie-rod; Axial force identification; Inverse problem; Dynamic test; Error analysis.

1 Introduction

In masonry buildings, metallic tie-rods are mainly used to inhibit the out-of-plane collapse of masonry walls (Sorrentino et al. 2017) or to resist the horizontal thrusts exerted by arches and vaults (Como 2013). In particular, the initial pretension of tie-rods can significantly reduce the force applied to the abutments by arches subjected to mere vertical loads (Giuriani et al. 2009). Vice versa, the tie-rod prestress scarcely influences the seismic capacity of an arch-pier system (Calderini and Lagomarsino, 2015, Calderini et al. 2015, Bolis et al. 2017). Nonetheless, the evaluation of the prestressing force of a tie-rod is of fundamental importance, especially when a restoration project is aimed at verifying or substituting single elements subjected to possible heavy decay (Bruschi et al. 2004, Gentile et al. 2017). To this end, static and dynamic methods have been proposed for the experimental evaluation of the axial load acting in tie-rods of arches and vaults, where the reference model was assumed to be a simply supported beam with rotational end constraints (Sorace 1996, Briccoli Bati and Tonietti 2001, Lagomarsino and Calderini 2005, Tullini and Laudiero 2008, Tullini, Rebecchi, and Laudiero 2012, Li et al. 2013, Gentilini, Marzano, and Mazzotti 2013, Campagnari et al. 2017). The introduction of elastic rotational end constraints is aimed at reproducing the restraining effect that the masonry offers to the part of the tie-rod embedded in the wall. More refined models made use of finite element based optimisation algorithms in which the unknown variables included the length of the tie-rod, concentrated masses and an elastic Winkler foundation simulating the interaction between the tie-rod and the masonry wall (Amabili et al. 2010, Garziera, Amabili, and Collini 2011, Ottoni and Blasi 2016, Collini. Garziera, and Riabova 2017). Unfortunately, in these approaches, nonuniqueness of estimated parameters may arise. As matter of fact, tie-rod extremities are embedded in masonry walls making doubtful the beam length and the location of the end constraints. To overcome this problem, Rebecchi (2011), Tullini (2013), Li et al. (2013), Rebecchi, Tullini, and Laudiero (2013) and Maes et al. (2013) proposed various methods to estimate the axial

force of tie-rods with unknown boundary conditions, where a tie-rod substructure of assigned length is adopted. These methods allow to overcome the difficulty of estimating the effective length free to vibrate, the boundary constraints, and the masses of the junction systems made to tighten the tie-rods, typical of ancient tie-rods. In fact, *in situ* tests may be performed on a tie-rod substructure located between the tightening systems. In particular, with laboratory test results as reference data, Rebecchi, Tullini, and Laudiero (2013) and Maes et al. (2013) estimated the axial force of a tie-rod with known geometric and elastic properties making use of one single vibration frequency and of five amplitudes of the corresponding mode shape. Nevertheless, in the case of hand-made ancient tie-rods, non homogeneities and non-uniform cross-sections may be present. Moreover, an experimental study on ancient tie-rods performed by Calderini et al. (2016) showed that a mean Young modulus E comparable to that of modern steel (209 GPa) may occur, but with a remarkable standard deviation of 76 GPa and a coefficient of variation about 36%. In any case, it is worth noting that the Young modulus can be evaluated by means of proper methods, like the experimental measurement of the longitudinal wave velocity (Boller, Chang, and Fujino 2009).

The procedure proposed in Tullini and Laudiero (2008) and Rebecchi, Tullini, and Laudiero (2013) was confirmed by several researches. For instance, Rainieri and Fabbrocino (2015) developed an automated operational modal analysis algorithm for vibration-based monitoring and tensile load estimation. Gentile et al. (2017) evaluated the axial force in 75 tie-rods of the Milan Cathedral. Cescatti et al. (2017) performed several numerical and experimental tests observing that relevant errors may occur for high values of the axial force only. This outcome is related to the difficulty of measuring small vibrations when increasing values of the axial force make the beam stiffer and stiffer (Tullini 2013, Rebecchi, Tullini, and Laudiero 2013). At the same time, the impact hammer force cannot be indefinitely increased if yielding has to be avoided.

Rainieri and Aenlle (2016) investigated the accuracy of the procedure for the tensile load estimation proposed in Rebecchi, Tullini, and Laudiero (2013). In particular, twenty-seven finite element models of tie-rods with various boundary conditions and various length and axial force values were investigated. The inaccuracy in the evaluation of the bending stiffness was considered by assuming a 14% underestimation of Young modulus (180 GPa instead of 210 GPa). The error in the evaluation of the material density was assumed to be equal to 0.6% (7800 kg/m^3 instead of 7850 kg/m^3). The influence of the input data errors on the axial load estimate turned out to be less than 14%. Moreover, making use of the reference values of the geometric and elastic properties, the influence of errors affecting the modal parameter estimation was investigated. An estimate error of ±1% affecting the fundamental frequency of the twenty-seven finite element models was considered first. In this case, the influence of measurement errors on axial load estimates was less than 4%. No analyses were made in the presence of errors affecting both input data and modal parameter estimates. Finally, it is worth noting that the procedures proposed in Rebecchi (2011), Tullini, Rebecchi, and Laudiero (2012), Tullini (2013) were also able to estimate compressive forces (Bonopera et al., 2018a, 2018b). Luong (2018) performed experimental modal testing on individual members of a historic Wiegmann–Polonceau truss to estimate the axial force. Nonetheless, a preliminary global analysis of the structure is required to identify potential local modes shapes at closely-spaced frequencies.

In the present paper, an investigation of the accuracy of the procedure for the tensile load estimation proposed in Tullini and Laudiero (2008), and Rebecchi, Tullini, and Laudiero (2013) is presented. In particular, the simplified procedure locating the mode shape amplitudes at the extremities, at the quarter sections and at midspan of the reference model was adopted. In this case, an explicit transcendental equation holds, depending on the axial force. In particular, the influence of measurement errors as well as of inaccurate estimates of the elastic properties on the accuracy of the axial force identification was considered by

means of many numerical tests. For the vibration frequencies and the mode shape amplitudes, measurement errors of ±1% were considered. For the Young modulus, an error of 15% with respect to the reference value E_{ref} = 206 GPa was assumed. Therefore, error analyses were performed assuming $E_{min} = 0.85 \cdot 206 = 175$ GPa and $E_{max} = 1.15 \cdot 206 = 237$ GPa. Comparisons were made with available experimental tests.

2 Axial load identification proposed by Rebecchi, Tullini, and Laudiero (2013)

A tie-rod reinforcing an arch-pier system is considered (Fig. 1a). The reference model is constituted by a prismatic beam of length L, located at any position between the relevant junction systems, and constrained by two sets of end elastic springs whose frequency-dependent parameters are collected by the 2×2 stiffness matrices $\mathbf{K}_0$ and $\mathbf{K}_1$ (Fig. 1b). The beam element is subjected to an axial force resultant N (tensile forces are assigned positive sign). Young's modulus E, mass per unit length m and cross-section second area moment J are assumed to be known constants.

The procedure proposed in Rebecchi, Tullini, and Laudiero (2013) can be simplified if one vibration frequency f and the corresponding mode shape amplitudes $v_i = v(x_i)$, for $i = 0, \ldots, 4$, are recorded at the five instrumented sections: $x_0 = 0$, $x_1 = L/4$, $x_2 = L/2$, $x_3 = 3L/4$ and $x_4 = L$. In this case, if the mid-section does not coincide with a node of the assumed mode shape, i.e. if $v_2 \neq 0$, the unknown parameter $n = NL^2/EJ$ can be obtained by solving the following transcendental equation:

$$\frac{v_1 + v_3}{v_2} = \frac{\dfrac{v_0 + v_4}{2v_2} + 1 + 2\cos\dfrac{q_1}{4}\cosh\dfrac{q_2}{4}}{\cos\dfrac{q_1}{4} + \cosh\dfrac{q_2}{4}} \tag{1}$$

where

$$q_1^2 = \frac{1}{2}\left(\sqrt{n^2 + 4\lambda^4} - n\right), \qquad q_2^2 = \frac{1}{2}\left(\sqrt{n^2 + 4\lambda^4} + n\right) = q_1^2 + n \tag{2a, b}$$

$$\lambda^4 = (2\pi f)^2 \frac{mL^4}{EJ}, \tag{2c}$$

It is worth noting that Eq. (1) does not require the knowledge of the boundary conditions. For simply supported beams, implying $v_0 = v_4 = 0$, Eq. (1) reduces to Eq. (16) reported in Tullini and Laudiero (2008). In summary, the axial force estimation is obtained according to the following steps:

- estimate one fundamental frequency f and the corresponding mode shape amplitudes v_0, v_1, v_2, v_3, v_4 by means of experimental modal analysis;
- compute λ by using Eq. (2c);
- solve the transcendental equation (1) for the unknown constant n by using the ratios $(v_1+v_3)/v_2$, $(v_0+v_4)/2v_2$ and the definitions for q_1 and q_2 in Eqs. (2a, b) where the value of λ is required;
- find the (analytical) axial force $N_a = n\, EJ/L^2$.

3 Experimental tests

In Rebecchi (2011), Rebecchi, Tullini, and Laudiero (2013), a set of experimental tests was developed (Figs. 2 and 3) to validate the analytical procedure illustrated in the previous section.

For a steel rod with a diameter of 20 mm, both Young's modulus ($E_{ref} = 206$ GPa) and density ($\rho_{ref} = 7850$ kg/m^3) were experimentally evaluated. In order to simulate end constraints of variable stiffness, the central span under examination, 3.00 m long, was prolonged with two outer spans with lengths $\overline{L}_0 = 1.16$ m and $\overline{L}_1 = 1.10$ m. Because of the difficulty in evaluating the effective rotational stiffness introduced by the experimental equipment, two springs of unknown stiffness k_s, k_d were idealized at the extremities of the three-span beam. Aimed at observing different interactions with the outer spans, a mass $\overline{m}$ was fixed at the mid-section of the span with length $\overline{L}_1$ (Figs. 2 and 3). In particular, it was assumed $\overline{m} = 0$ kg for tests No. 1 and 2, $\overline{m} = 20$ kg for test No. 3 and 4, and $\overline{m} = 10$ kg for tests No. 5 and 6. In tests No. 1, 3, 5, sensors spaced of $L/4 = 0.75$ m were used, whereas in

tests No. 2, 4, 6, the outer accelerometers were placed at distances $L_0 = L_1 = 0.30$ m from the ends to obtain a reference model with length $L = 2.4$ m. Details of test rig and experimental setup can be found in Tullini and Laudiero (2008), Rebecchi (2011), Rebecchi, Tullini, and Laudiero (2013).

For each value of the imposed axial load N_x, the experimental tests were performed three times, hitting each of the instrumented sections of the central span. Consequently, 15 tests were collected for each value of N_x in the configurations No. 2, 4, 6. With reference to the first mode shape of test No. 2, Table 1 shows the coefficient of variation (CoV) of the experimental parameters for each value of N_x. Unavoidable differences in repeated tests yield a CoV for experimental values of N_x as well. The CoV of the frequency f never exceeds the value of 0.24%, with a corresponding CoV of λ less than 0.12%. The CoV of the ratio $(v_0+v_4)/2v_2$ is less than 0.31% even though the CoV of the ratio v_0/v_2 rises up to 0.64%. The maximum value of the CoV of ratio $(v_1+v_3)/2v_2$ is equal to 0.22%. The CoV of the analytical estimates N_a of the axial loads is less than 1.4% for $N_x > 10$ kN.

As reported in Rebecchi (2011), Rebecchi, Tullini, and Laudiero (2013), the first mode shape of tests No. 3 and 4 exhibits a significant scattering in modal data. For test No. 4, this behaviour is confirmed by the CoV values shown in Table 2, where a CoV of the ratio $(v_1+v_3)/2v_2$ of about 1% gives rise to a CoV of 10% for N_a that rises up to 25% for a CoV of the ratio $(v_1+v_3)/2v_2$ of about 3%.

4 Numerical simulations and error analyses

With reference to the tests reported in the previous section, the influence of measurement errors as well as of inaccurate estimates of the elastic properties on the accuracy of the axial force identification was considered. The effect of the added mass of the sensors was also analyzed. To this end, a finite element model of the continuous beam representing the experimental setup of Figs. 2 and 3 was developed by using the commercial Finite Element Software Midas/Gen (2018), where the classic geometric stiffness matrix was adopted

(Bazant and Cedolin 1991). The middle span was meshed with 64 finite elements, whereas for each additional span 22 finite elements were adopted. The end stiffnesses k_s, k_d were set equal to zero. The assigned values of the axial load were assumed to be 5, 10, 15, 20, 30, 40, 50 kN and are denoted by N_x in the following. The analytical estimates N_a of the axial loads were determined by solving Eq. (1) for each set of the numerical data [λ, $(v_0+v_4)/2v_2$, $(v_1+v_3)/2v_2$]. Comparisons were made with the experimental results reported in Rebecchi (2011), Rebecchi, Tullini, and Laudiero (2013).

For vibration frequencies and mode shape amplitudes, measurement errors of ±1% were adopted to perturb the numerical values of each modal deflection and the corresponding frequency. In particular, the set of numerical data [f, v_0, …, v_4] were multiplied by [1.01, …, 1.01], [1.01, …, 0.99], …, [0.99, …, 0.99]. Consequently, the three sensors used in test configurations No. 1, 3, 5 (Fig. 2) gave rise to 16 different combinations of simulated experimental values for 7 distinct values of the axial force N_x. Analogously, the five sensors employed in tests No. 2, 4, 6 (Fig. 3) lead to 64 × 7 different combinations of numerical values. As suggested in Rebecchi (2011), Rebecchi, Tullini, and Laudiero (2013), the second mode shape was used in tests No. 2 and 4, whereas the first mode shape was used in the other tests. In fact, for $\overline{m} \leq 10$ kg, the first mode shape of the whole system is mainly governed by flexural deformations of the central span, see Fig. 12b in Rebecchi, Tullini, and Laudiero (2013). Vice versa, for $\overline{m} = 20$ kg, the analogous mode shape is the second one, see Fig. 12c in Rebecchi, Tullini, and Laudiero (2013), whereas the first mode shape is mainly ruled by the translational motion of the additional mass. Thus, small displacements in the central beam arise and the first peak amplitude may be one hundredth of the second one. This behaviour arises in the presence of high values of the axial force.

For each value assumed for the axial force N_x, the worst analytical estimate for N_a was searched and retained. As discussed in the previous section, measurement errors of ±1% resulted to be a severe assumption. In fact, the CoV of the three experimental data [λ,

$(v_0+v_4)/2v_2$, $(v_1+v_3)/2v_2$] to be used in Eq. (1) is less than half of the CoV of the single measurement error.

4.1 Influence of Young modulus

For the Young modulus, an error of 15% with respect to the reference value E_{ref} = 206 GPa was assumed. Then, error analyses were performed assuming $E_{min} = 0.85 \cdot 206 = 175$ GPa and $E_{max} = 1.15 \cdot 206 = 237$ GPa. The mass of the sensors was neglected in the error analyses of this section. Figs. 4 and 5 show the ratio between the worst estimated values N_a and the assumed values N_x of the axial forces for tests No. 1, 3, 5 and No. 2, 4, 6, respectively. As expected, estimated values of tests No. 1, 3, 5 are better than those of tests No. 2, 4, 6. Nonetheless, all test configurations yield good axial force estimates for $N_x > 20$ kN irrespective of the adopted Young modulus. Thus, analytical estimates N_a are mainly affected by measurement errors. It is worth noting that the experimental tests performed in Rebecchi (2011), Rebecchi, Tullini, and Laudiero (2013) provided for excellent axial force estimations for all values of N_x (symbols + in Figs. 4 and 5), even though no high precision experimental apparatus was used. Therefore, the reliability of the tensile force identification in ancient tie-rods relies on the correct estimation of measurement errors involved in the experimental modal analysis rather than on accurate guess of Young modulus. To highlight this aspect, Young modulus E_{ref} and measurement errors of ±1.0% and ±0.5% were adopted. The worst ratio N_a/N_x obtained is reported in Fig. 6 showing that the errors in the analytical estimates adopting measurement errors of ±0.5% became about a half of those with errors ±1.0%.

4.2 Influence of sensor mass

Each sensor employed in the experimental tests has a weight of 40 g, including the metallic wrappers used to fasten the accelerometers to the beam. Thus, for tests No. 2, 4, 6 the total weight of the sensors was equal to 0,2 kg, whereas the weight of central span of the beam is

7.4 kg, corresponding to a weight ratio of 2.7%. If the total mass of the sensors is distributed along the beam, a modified beam density ρ_{mod} = 8062 kg/m^3 is obtained.

To describe the influence of the sensor mass on the axial load estimation, the accelerometers were initially modeled in the finite element model as concentrated masses located at the instrumented sections. Nonetheless, no significant differences were obtained using a uniform beam with modified beam density ρ_{mod}. Fig. 6 shows the ratio between the worst estimated values N_a and the assumed values N_x of the axial forces for tests No. 2, 4, 6, adopting modified density ρ_{mod} and Young modulus E_{ref} with measurement errors of ±1.0% and ±0.5%. Moreover, Fig. 6 shows data from experimental tests evaluated using ρ_{mod}. For tests No. 2 and 6, the average percent error between the mean value for N_a and the assigned forces N_x resulted to be less than 0.6% for N_x > 5 kN whereas, for tests no. 4, the average percent error was less than 0.6% for N_x > 15 kN. Conversely, for all tests, the average percent error turned out to be about 2.5% when ρ_{ref} was adopted (Rebecchi, Tullini, and Laudiero (2013).

4.3 Influence of sensor position

With reference to test no. 1, in the numerical model the error in the sensor position was represented by displacing sensors 1 and 3 of 3 mm giving a ratio 0.03/(3.00/4) = 0.4%. No appreciable variation in the axial load estimate occurred if both sensors were shifted in the same direction. Vice versa, the average percent error of the mean values N_a and the assigned forces N_x almost reached the value of 1.2% for N_x > 10 kN if sensors were shifted in the opposite directions. However, error in sensor position may be included in the measurement error on mode shape amplitude.

5 Practical aspects

In the field of experimental modal analysis, uncertainty bounds for the modal parameter estimates can be obtained by means of advanced identification techniques such as the

stochastic subspace identification method (Peeters and De Roeck 2001, Reynders and De Roeck 2008, Reynders et al. 2008, 2016). Alternatively, repeated experimental tests can be used to evaluate the CoV of the parameters to be used in Eq. (1).

The three-span beam shown in Figs. 2 and 3 may also be representative of real tie-rods. In fact, intermediate supports were possibly used to sustain long tie-rods, as in the case of the tie-rods of Parma Cathedral (Garziera, Amabili, and Collini 2011), and the concentrated mass $\overline{m}$ simulates the presence of heavy lamps hanging from the tie-rod (Gentile et al., 2017). In all these cases, experimental tests can be performed on a proper tie-rod substructure of assigned length, but the flexural mode shape to be used in the identification process has to be properly selected. To this respect, see section 5.2 in Rebecchi, Tullini, and Laudiero (2013), where several suggestions were outlined. For instance, mode shapes with amplitudes v_0, v_1, v_2, v_3, v_4 with the same sign, showing the maximum amplitude v_2, have to be preferred in the identification process. Vice versa, local mode shapes close to a straight line have to be systematically eliminated.

For a beam with severe cross section variations, a finite element model can be helpful for the determination of the optimal uniform beam approximating the frequencies of the irregular beam.

It is worth noting that tie-rod vibrations can also be measured using non-contact vibration techniques (Gioffré et al. 2017). Non-contact measurement systems received considerable interest in the last decades (Pieraccini et al. 2000, 2007, 2014, Gentile 2010). In fact, non-contact measurements are very attractive in case of tie-rods hardly accessible.

Conclusions

An investigation into the reliability of an experimental procedure for the axial load identification of tie-rods, using one flexural mode shape, was presented. Flexural rigidity and mass per unit length were assumed to be known constants. Then, the influence of inaccurate estimates of geometric and elastic properties as well as of measurement errors on the accuracy

of the axial force identification was investigated. Many numerical tests on tie-rods having large scatter values of elastic properties were performed. Good estimates of the axial forces were obtained, and the reliability of the tensile force identification was shown to rely on the correct estimation of measurement errors rather than on accurate guess of Young modulus.

In summary, the recommended scheme for *in situ* experiments is the following:

- use the five sensors test when it is difficult to estimate the effective length free to vibrate, the boundary constraints, and the masses of the junction systems; vice versa, the three sensors test leads to more accurate results;
- estimate Young modulus by measuring the longitudinal wave velocity (Boller, Chang, and Fujino 2009);
- repeat tests for a proper evaluation of the coefficient of variation of the modal data to be used in the identification process. In fact, excellent estimates of the axial forces are obtained when the experimental ratios $(v_0+v_4)/2v_2$, $(v_1+v_3)/2v_2$ have a coefficient of variation less than 0.5%;
- use a modified beam density ρ_{mod} by distributing the total mass of the sensors along the beam length;
- make sure the sensor location error be less than 0.5% of $L/4$.

Acknowledgments

The present investigation was developed in the framework of the Research Program FAR 2018 of the University of Ferrara.

References

Amabili, M., S. Carra, L. Collini, R. Garziera, and A. Panno. 2010. Estimation of tensile force in tie-rods using a frequency-based identification method. *Journal of Sound and Vibration* 329 (11):2057–67. doi: 10.1016/j.jsv.2009.12.009.

Bazant, Z. P., and L. Cedolin. 1991. *Stability of Structures*. New York: Oxford University Press.

Bolis, V., M. Preti, A. Marini, and E. Giuriani. 2017. Experimental cyclic and dynamic in-plane rocking response of a masonry transverse arch typical of historical churches. *Engineering Structures* 147:285–296. doi: 10.1016/j.engstruct.2017.05.058.

Boller, C., F.-K. Chang, Y. Fujino (Eds.). 2009. *Encyclopaedia of Structural Health Monitoring*. Chichester: John Wiley & Sons, Ltd.

Bonopera, M., K.-C. Chang, C.-C. Chen, Z.-K. Lee, and N. Tullini. 2018a. Axial load detection in compressed steel beams using FBG–DSM sensors. *Smart Structures and Systems* 21(1):53–64. doi: 10.12989/sss.2018.21.1.053.

Bonopera, M., K.-C. Chang, C.-C. Chen, T.-K. Lin, and N. Tullini. 2018b. Compressive column load identification in steel space frames using second-order deflection-based methods. *International Journal of Structural Stability and Dynamics* 18 (8): Article number 1850092, 1–16. doi: 10.1142/S021945541850092X.

Briccoli Bati, S., and U. Tonietti. 2001. Experimental methods for estimating in situ tensile force in tie-rods. *Journal of Engineering Mechanics* 127 (12):1275–83. doi: 10.1061/(ASCE)0733-9399(2001)127:12(1275).

Bruschi, G., G. Nardoni, L. Lanza, F. Laudiero, N. Tullini, G. Mezzadri, and S. Tralli. 2004. Experimental stress analysis of historical forged tie beams of archaeological museum of Spina in Ferrara, Italy. In *Proceedings of Structural Analysis of Historical Constructions*, Eds. C. Modena, P.B. Lourenço and P. Roca Vol. 1, 489–497. London: Taylor & Francis.

Calderini, C., and S. Lagomarsino. 2015. Seismic response of masonry arches reinforced by tie-rods: Static tests on a scale model. *Journal of Structural Engineering* 141 (5): Article number 4014137. doi: 10.1061/(ASCE)ST.1943-541X.0001079.

Calderini, C., S. Lagomarsino, M. Rossi, G. Decanio, M. Mongelli and I. Roselli. 2015. Shaking table tests of an arch-pillars system and design of strengthening by the use of tie-rods. *Bulletin of Earthquake Engineering* 13 (1):279–97. doi: 10.1007/s10518-014-9678-x.

Calderini, C., R. Vecchiattini, C. Battini, and P. Piccardo. 2016. Mechanical and metallographic characterization of iron tie-rods in masonry buildings: An experimental study. In *Proceedings of the 10th International Conference on Structural Analysis of Historical Constructions, SAHC 2016*, Eds. K. Van Balen and E. Verstrynge, 1293–00. Leuven: CRC Press.

Campagnari, S., F. Di Matteo, S. Manzoni, M. Scaccabarozzi, and M. Vanali. 2017. Estimation of axial load in tie-rods using experimental and operational modal analysis. *Journal of Vibration and Acoustics, Transactions of the ASME*. 139 (4): Article number 041005. doi: 10.1115/1.4036108.

Cescatti, E., F. da Porto, C. Modena, and F. Casarin. 2017. Ties in historical constructions: Typical features and laboratory tests. In *Proceedings of the 10th International Conference on Structural Analysis of Historical Constructions, SAHC 2016*, Eds. K. Van Balen and E. Verstrynge, 1301–07. Leuven: CRC Press.

Collini, L., R. Garziera, and K. Riabova. 2017. Vibration analysis for monitoring of ancient tie-rods. *Shock and Vibration* 2017: Article number 7591749. doi: 10.1155/2017/7591749.

Como, M. 2013. *Statics of historic masonry constructions*. Berlin: Springer.

Garziera, R., M. Amabili, and L. Collini. 2011. A hybrid method for the nondestructive evaluation of the axial load in structural tie-rods. *Nondestructive Testing and Evaluation* 26 (2):197–208. doi: 10.1080/10589759.2011.556728.

Gentile, C. 2010. Deflection measurement on vibrating stay cables by non-contact microwave interferometer. *NDT & E International* 43 (3):231–40. doi: 10.1016/j.ndteint.2009.11.007.

Gentile, C., C. Poggi, A. Ruccolo, and M. Vasic. 2017. Dynamic assessment of the axial force in the tie-rods of the Milan Cathedral. *Procedia Engineering* 199:3362–67. doi: 10.1016/j.proeng.2017.09.442.

Gentilini, C., A. Marzani, and M. Mazzotti. 2013. Nondestructive characterization of tie-rods by means of dynamic testing, added masses and genetic algorithms. *Journal of Sound and Vibration* 332 (1):76–101. doi: 10.1016/j.jsv.2012.08.009.

Gioffré, M., N. Cavalagli, C. Pepi, and M. Trequattrini. 2017. Laser doppler and radar interferometer for contactless measurements on unaccessible tie-rods on monumental buildings: Santa Maria della Consolazione Temple in Todi. *Journal of Physics: Conference Series* 778(1): Article number 012008.

Giuriani, E., A. Marini, C. Porteri, and M. Preti. 2009. Seismic vulnerability for churches in association with transverse arch rocking. *International Journal of Architectural Heritage* 3 (3):212–34. doi: 10.1080/15583050802400240.

Lagomarsino, S., and C. Calderini. 2005. The dynamical identification of the tensile force in ancient tie-rods. *Engineering Structures* 27 (6):846–56. doi: 10.1016/j.engstruct.2005.01.008.

Li, S., E. Reynders, K. Maes, and G. De Roeck. 2013. Vibration-based estimation of axial force for a beam member with uncertain boundary conditions. *Journal of Sound and Vibration* 332 (4):795–806. doi: 10.1016/j.jsv.2012.10.019.

Luong, H.T.M. 2018. Identification of the state of stress in iron and steel truss structures by vibration-based experimental investigations. PhD Thesis. Bundesanstalt für Materialforschung und -prüfung (BAM), Berlin, Germany. https://opus4.kobv.de/opus4-bam/frontdoor/index/index/docId/44961.

Maes, K., J. Peeters, E. Reynders, G. Lombaert, and G. De Roeck. 2013. Identification of axial forces in beam members by local vibration measurements. *Journal of Sound and Vibration* 332 (21):5417–32. doi: 10.1016/j.jsv.2013.05.017.

Midas/Gen. 2018. http://en.midasuser.com (accessed December 28, 2017).

Ottoni, F., and C. Blasi. 2016. Hooping as an ancient remedy for conservation of large masonry domes. 10 (2-3):164–81, doi: 10.1080/15583058.2015.1113335.

Peeters, B., and G. DeRoeck. 2001. Stochastic system identification for operational modal analysis: a review. *Journal of Dynamic Systems, Measurement, and Control* 123 (4):659–67. doi: 10.1115/1.1410370.

Pieraccini, M., D. Tarchi, H. Rudolf, D. Leva, G. Luzi, G. Bartoli, and C. Atzeni. 2000. Structural static testing by interferometric syntethic radar. *NDT & E International* 33 (8):565–70. doi: 10.1016/S0963-8695(00)00027-X.

Pieraccini, M., F. Parrini, D. Dei, M. Fratini, C. Atzeni, and P. Spinelli. 2007. Dynamic characterization of a bell-tower by interferometric sensor. *NDT & E International* 40 (5):390–96. doi: 10.1016/j.ndteint.2006.12.010.

Pieraccini, M., D. Dei, M. Betti, G. Bartoli, G. Tucci. and N. Guardini. 2014. Dynamic identification of historic masonry towers through an expeditious and no-contact approach: application to the "Torre del Mangia" in Siena (Italy). *Journal of Cultural Heritage* (15):275–85. doi: 10.1016/j.culher.2013.07.006.

Sorace, S. 1996. Parameter models for estimating in-situ tensile force in tie-rods, *Journal of Engineering Mechanics* 122 (9):818–25. doi: 10.1061/(ASCE)0733-9399(1996)122:9(818).

Rainieri, C., and M. L. Aenlle. 2016. The influence of parameter estimation error on the accuracy of a vibration based tensile load estimation technique. In *Proceedings of ISMA 2016 - International Conference on Noise and Vibration Engineering and USD2016 - International Conference on Uncertainty in Structural Dynamics.* 1697–1710. Leuven: ISMA.

Rainieri, C., and G. Fabbrocino. 2015. Development and validation of an automated operational modal analysis algorithm for vibration-based monitoring and tensile load estimation. *Mechanical Systems and Signal Processing* 60-61:512–34. doi: 10.1016/j.ymssp.2015.01.019.

Rebecchi, G. 2011. *Beam axial load identification using one vibration mode shape*, PhD Thesis, University of Ferrara. http://eprints.unife.it/tesi/389.

Rebecchi, G., N. Tullini, and F. Laudiero. 2013. Estimate of the axial force in slender beams with unknown boundary conditions using one flexural mode shape. *Journal of Sound and Vibration* 332 (18):4122–35. doi: 10.1016/j.jsv.2013.03.018.

Reynders, E., and G. De Roeck. 2008. Reference-based combined deterministic–stochastic subspace identification for experimental and operational modal analysis. *Mechanical Systems and Signal Processing* 22 (3):617–37. doi: 10.1016/j.ymssp.2007.09.004.

Reynders, E., R. Pintelon, and G. De Roeck. 2008. Uncertainty bounds on modal parameters obtained from stochastic subspace identification. *Mechanical Systems and Signal Processing* 22 (4):948–69. doi: 10.1016/j.ymssp.2007.10.009.

Reynders, E., K. Maes, G. Lombaert, and G. De Roeck. 2016. Uncertainty quantification in operational modal analysis with stochastic subspace identification: Validation and applications. *Mechanical Systems and Signal Processing* 66–67 (1):13–30. doi: 10.1016/j.ymssp.2015.04.018.

Sorrentino, L., D. D'Ayala, G. de Felice, M. C. Griffith, S. Lagomarsino, and G Magenes. 2017. Review of out-of-plane seismic assessment techniques applied to existing masonry buildings. *International Journal of Architectural Heritage* 11 (1):2–21.doi: 10.1080/15583058.2016.1237586.

Tullini, N. 2013. Bending tests to estimate the axial force in slender beams with unknown boundary conditions. *Mechanics Research Communications* 53:15–23. doi: 10.1016/j.mechrescom.2013.07.011.

Tullini, N., and F. Laudiero. 2008. Dynamic identification of beam axial loads using one flexural mode shape. *Journal of Sound and Vibration* 318 (1-2):131–47. doi: 10.1016/j.jsv.2008.03.061.

Tullini, N., G. Rebecchi, and F. Laudiero. 2012. Bending tests to estimate the axial force in tie-rods. *Mechanics Research Communications* 44:57–64. doi: 10.1016/j.mechrescom.2012.06.005.

Figure Captions

Figure 1. Arch-pier system reinforced with a tie-rod having two junction systems (a) and reference model with location of the instrumented sections (b).

Figure 2. Experimental setup for tests No. 1, 3, 5.

Figure 3. Experimental setup for tests No. 2, 4, 6.

Figure 4. Tests No. 1, 3, 5. Ratio between the worst estimated values (N_a) and the assumed values (N_x) of the axial forces for tie-rods with Young modulus $E_{\min}$ (dashed line), $E_{\max}$ (dash dot line) and E_{ref} (continuous line). Symbols + refer to data from experimental tests.

Figure 5. Tests No. 2, 4, 6. Ratio between the worst estimated values (N_a) and the assumed values (N_x) of the axial forces for tie-rods with Young modulus $E_{\min}$ (dashed line), $E_{\max}$ (dash dot line) and E_{ref} (continuous line). Symbols + refer to data from experimental tests.

Figure 6. Tests No. 2, 4, 6. Ratio between the worst estimated values (N_a) and the assumed values (N_x) of the axial forces for tie-rods with modified density $\rho_{\text{mod}} = 8062$ kg/m^3 and with E_{ref} affected by measurement errors of ±1.0% (continuous line) and ±0.5% (continuous line with symbols). Symbols + refer to data from experimental tests evaluated using ρ_{mod}.

Table Captions

Table 1. Test No. 2 ($\overline{m}$ = 0 kg). Imposed axial load N_x and coefficients of variation (CoV) of the experimental parameters and of analytical estimate N_a for the first mode shape.

Table 2. Test No. 4 ($\overline{m}$ = 20 kg). Imposed axial load N_x and coefficients of variation (CoV) of the experimental parameters and of analytical estimate N_a for the first mode shape.

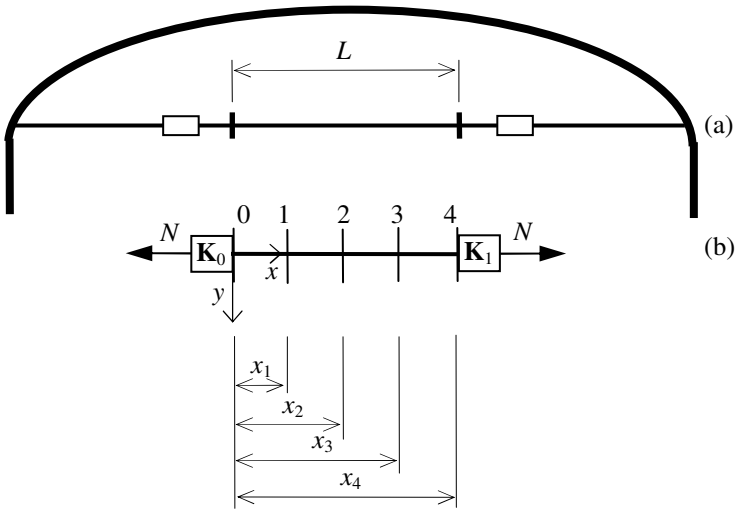

Figure 1. Arch-pier system reinforced with a tie-rod having two junction systems (a) and reference model with location of the instrumented sections (b).

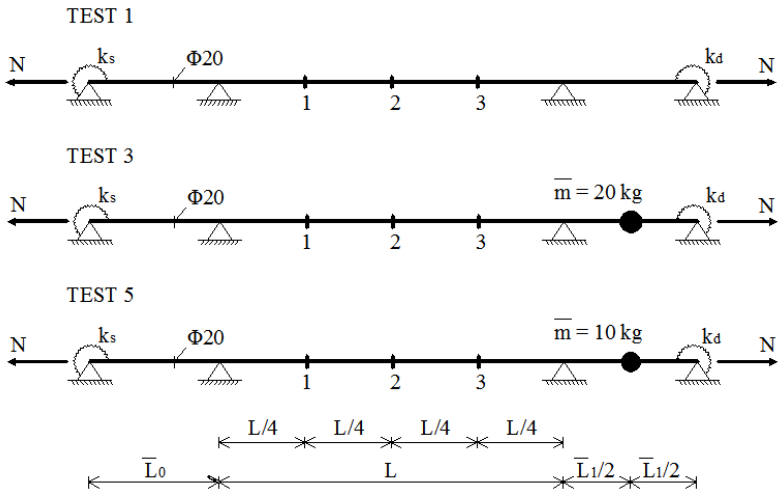

Figure 2. Experimental setup for tests No. 1, 3, 5.

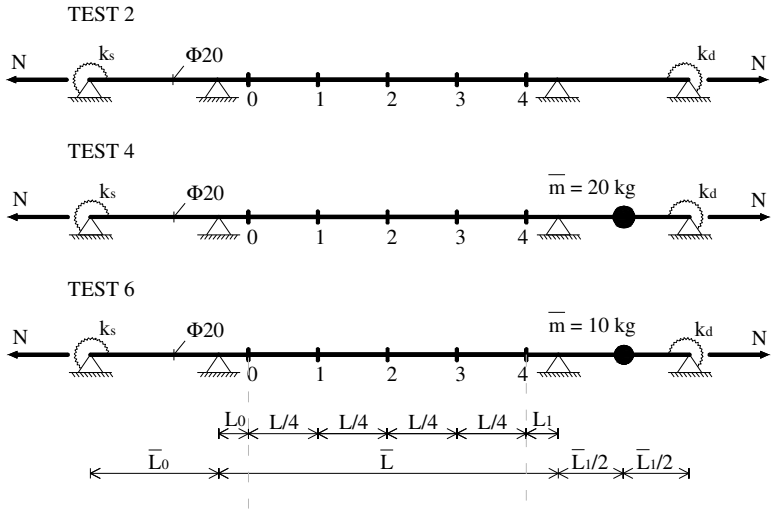

Figure 3. Experimental setup for tests No. 2, 4, 6.

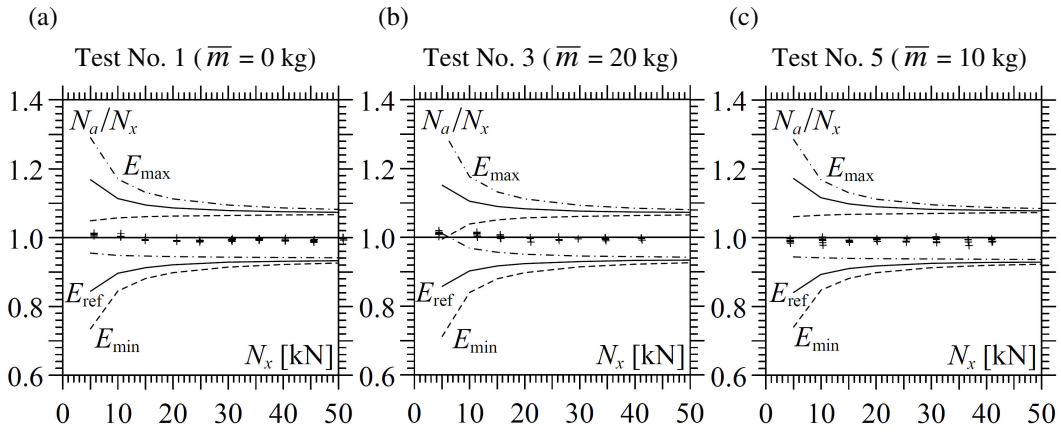

Figure 4. Tests No. 1, 3, 5. Ratio between the worst estimated values (N_a) and the assumed values (N_x) of the axial forces for tie-rods with Young modulus E_{min} (dashed line), E_{max} (dash dot line) and E_{ref} (continuous line). Symbols + refer to data from experimental tests.

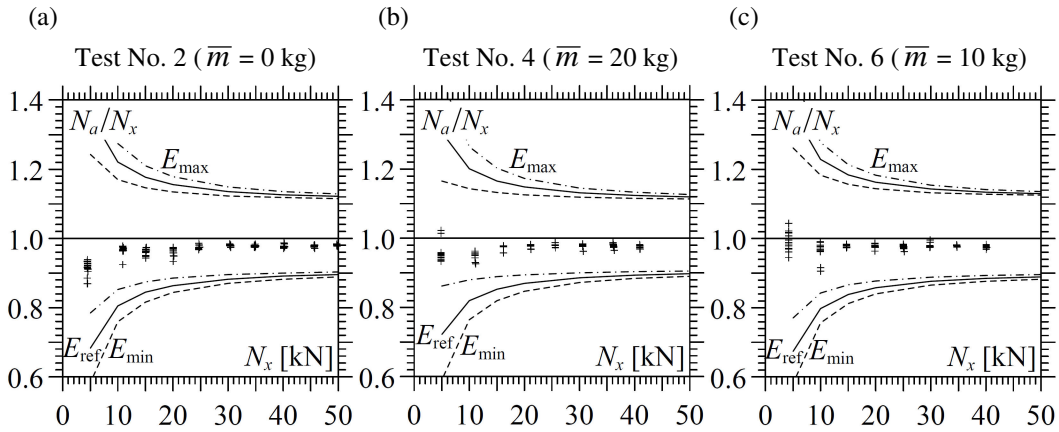

Figure 5. Tests No. 2, 4, 6. Ratio between the worst estimated values (N_a) and the assumed values (N_x) of the axial forces for tie-rods with Young modulus E_{min} (dashed line), E_{max} (dash dot line) and E_{ref} (continuous line). Symbols + refer to data from experimental tests.

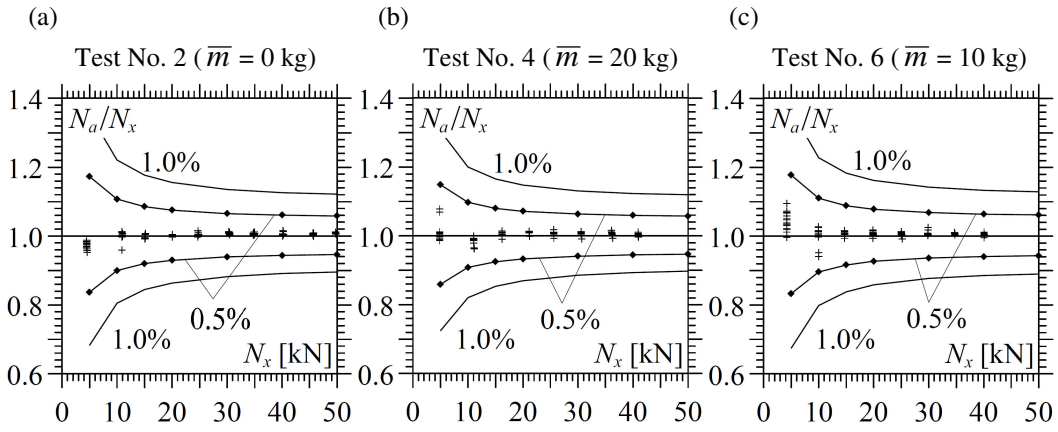

Figure 6. Tests No. 2, 4, 6. Ratio between the worst estimated values (N_a) and the assumed values (N_x) of the axial forces for tie-rods with modified density ρ_{mod} = 8062 kg/m^3 and with E_{ref} affected by measurement errors of ±1.0% (continuous line) and ±0.5% (continuous line with symbols). Symbols + refer to data from experimental tests evaluated using ρ_{mod}.

Table 1. Test No. 2 ($\overline{m}$ = 0 kg). Imposed axial load N_x and coefficients of variation (CoV) of the experimental parameters and of analytical estimate N_a for the first mode shape.

N_x	CoV [%]									
[kN]	N_x	f	v_0/v_2	v_1/v_2	v_3/v_2	v_4/v_2	λ	$(v_1+v_3)/2v_2$	$(v_0+v_4)/2v_2$	N_a
4.50	1.14	0.00	0.48	0.23	0.09	0.26	0.00	0.14	0.31	2.6
10.9	0.43	0.19	0.64	0.28	0.14	0.23	0.10	0.16	0.31	1.4
15.1	0.26	0.24	0.36	0.27	0.12	0.21	0.12	0.10	0.17	1.1
20.1	0.16	0.17	0.33	0.49	0.09	0.14	0.09	0.22	0.13	1.1
24.7	0.24	0.20	0.37	0.11	0.14	0.22	0.10	0.06	0.17	0.7
30.4	0.20	0.09	0.25	0.08	0.09	0.27	0.05	0.04	0.18	0.2
34.9	0.21	0.15	0.17	0.10	0.08	0.08	0.08	0.03	0.09	0.3
40.2	0.12	0.16	0.19	0.08	0.10	0.14	0.08	0.06	0.11	0.5

Table 2. Test No. 4 ($\overline{m}$ = 20 kg). Imposed axial load N_x and coefficients of variation (CoV) of the experimental parameters and of analytical estimate N_a for the first mode shape.

N_x	CoV [%]					
[kN]	N_x	f	λ	$(v_1+v_3)/2v_2$	$(v_0+v_4)/2v_2$	N_a
4.90	0.26	0.00	0.00	0.20	0.42	3.2
11.1	0.34	0.00	0.00	0.37	0.42	3.8
16.2	0.03	0.00	0.00	0.18	0.52	1.5
21.1	0.09	0.00	0.00	0.45	0.46	4.0
25.6	0.29	0.00	0.00	1.24	4.04	10.4
30.6	0.06	0.00	0.00	0.28	0.28	2.4
36.2	0.10	0.00	0.00	1.10	0.99	9.2
41.0	0.10	0.00	0.00	3.16	1.48	25.0